A Rigorous Three Plane Mode-Matching Technique for Characterizing Waveguide T-Junctions, and its Application in Multiplexer Design

Xiao-Peng Liang, *Student Member, IEEE*, Kawthar A. Zaki, *Fellow, IEEE*, and Ali E. Atia, *Fellow, IEEE*

Abstract—**A rigorous method for modeling rectangular waveguide T-junctions is presented. The method characterizes the waveguide discontinuity three times when the side-arm of the T-junction is terminated in a short circuit with three different lengths, and hence is called the three plane mode-matching technique (TPMMT). Computed and measured data on both *E*-plane and *H*-plane T-junctions are compared, showing excellent agreement for the magnitudes and phases of the scattering matrix elements. Element values of equivalent circuit models proposed by Marcuvitz [6] are computed and approximated by simple polynomials or rational functions, giving excellent accuracy. By using the *S*-parameters obtained from the TPMMT method, a network model of a waveguide manifold multiplexer is formulated. All parameters of the multiplexer, including the manifold dimensions and the filters, are optimized using this network model in terms of the multiplexer specification. The experimental results match the computed optimum results without further adjustment.**

I. Introduction

WAVEGUIDE T-junctions play an important role in designing microwave circuits, such as multiplexers used in modern communication systems [1]–[4], and power dividers [5]. Modeling waveguide T-junctions is an old problem. Initially, equivalent circuits were derived based on electrostatic approximations [6]. These approximations do not give sufficiently accurate results for many applications. In recent years, the finite element method (FEM) and the boundary element method (BEM) have been applied to solve this problem, and gave very good results [7]. However, these methods require considerable computing effort.

Mode-matching techniques have been used in the past for the solution of a wide range of waveguide discontinuity problems. For mode matching to be valid, the geometry of the configuration must have proper boundaries to allow the division of the structure into regions, the expansions of the fields in terms of natural modes in each region, and then the infinite set of mode-matching equations can be truncated to a finite set and solved numerically. If the field representation in any region cannot be expanded in terms of natural modes, mode matching will be invalid [8]. Unfortunately waveguide T-junctions have a region (Region 4 in Fig. 1(a)) where the fields cannot be expanded in terms of natural modes.

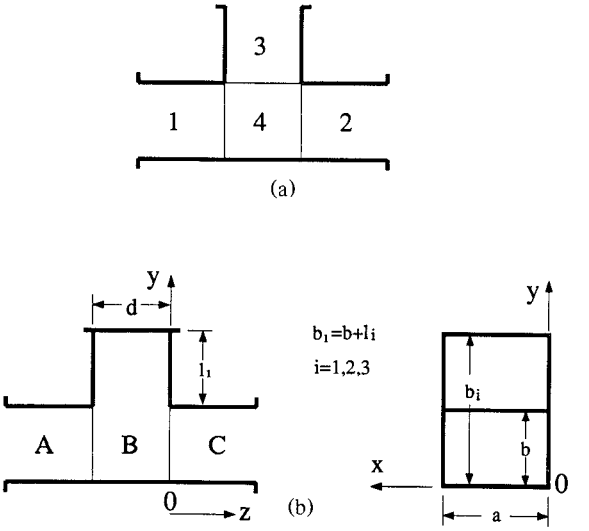

Fig. 1. The cross sections of T-junction and side-arm shorted T-junction.

One approach, introduced in the late 1960's [9], uses equivalent-circuit concepts applied to waveguide modes. This method calculates the admittance matrix of the T-junction by successively placing short circuits exactly at two of the three openings of the T-junction (i.e., at the thin lines in Fig. 1(a)), yielding three one ports consisting of shorted uniform waveguides. The same strategy is used in [4], [5] to compute the scattering matrix of the T-junction.

This paper uses the mode-matching technique directly, by modifying the configuration to avoid the field defective regions. The method modifies the configuration by plac-

Manuscript received March 15, 1991; revised July 6, 1991.

X-P. Liang and K. A. Zaki are with the Electrical Engineering Department, University of Maryland, College Park, MD 20742.

A. E. Atia is with COMSAT Systems Division, 22300 Comsat Drive, Clarksburg, MD 20871.

IEEE Log Number 9102779.

ing a short circuit on the side arm of the T-junction some distance away from the discontinuity. The scattering matrix of the resulting two-port network is then computed rigorously by mode matching. By repeating the same process with three different positions of the short circuit on the side arm, the three-port scattering matrix of the T-junction can be extracted. Since the solution is obtained by using mode matching three times, the method proposed will be called the three plane mode-matching technique (TPMMT).

The computed results using the TPMMT were verified by experimental measurements, and excellent agreement was obtained for both the magnitudes and phases of all the scattering matrix elements of both *E*- and *H*-plane T-junctions.

Accurate circuit models of T-junctions suitable for use in CAD programs are derived. The topologies of the models are the same as those introduced by Marcuvitz [6]; however, the element values are derived as simple polynomials or rational functions of frequency, from the scattering matrix obtained from the TPMMT.

Using the T-junctions model from the TPMMT, a network model of a manifold type multiplexer is developed. The dimensions of the manifold and the coupling parameters of the filters are optimized on this network model in terms of the multiplexer specification. An example 4-channel *S*-band multiplexer is built in accordance with the optimized design. Each of the four filters was built and tuned separately to its optimized response, and the multiplexer was then assembled as a five-port network. The computed and measured results agreed remarkably without further adjustment.

II. Three Plane Mode-Matching Technique (TPMMT)

A. Three Plane Measurement Method

A waveguide T-junction is modeled by a three-port network as shown in Fig. 2(a). We developed a method, called three plane measurement method, to measure the scattering parameters of this three-port network by a network analyzer. The method can be described as follows. 1) Connect three short circuits, (one at a time), with reflection coefficient $e^{j\theta_i}$ $(i=1,2,3)$ to one of the three ports (port 3). 2) Measure the *S*-parameters of each of the resulting two-port networks $[S_{mi}]$, $i=1,2,3$, (port 1 to port 2) by a network analyzer (Fig. 2(b)). Let these two port parameters be

$$[S_{mi}]=\begin{bmatrix} S_{m11i} & S_{m12i} \\ S_{m21i} & S_{m22i} \end{bmatrix}, \qquad i=1,2,3. \tag{1}$$

3) Calculate the *S*-parameters of the three-port network from the three measured two-port network *S*-parameters. Assuming the three-port network *S*-parameters are

$$[S]=\begin{bmatrix} S_{11} & S_{12} & S_{13} \\ S_{21} & S_{22} & S_{23} \\ S_{31} & S_{32} & S_{33} \end{bmatrix}. \tag{2}$$

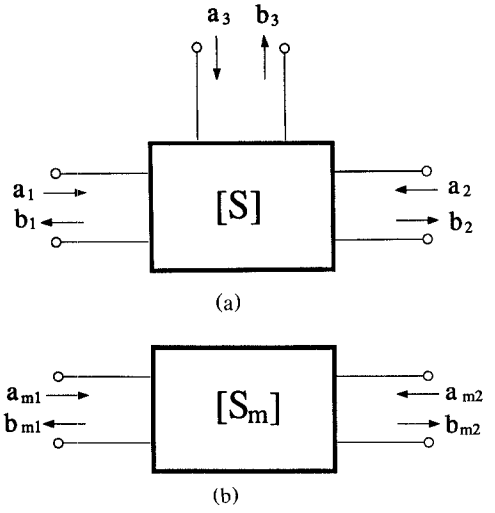

Fig. 2. Three-port and two-port networks.

Then, the relationship between $[S]$ and $[S_{mi}]$ can be easily derived:

$$S_{m11i}=S_{11}+\frac{S_{31}^2 e^{j\theta_i}}{1-S_{33}e^{j\theta_i}}, \qquad i=1,2,3 \tag{3a}$$

$$S_{m21i}+S_{21}=\frac{S_{31}^2 e^{j\theta_i}}{1-S_{33}e^{j\theta_i}}, \qquad i=1,2,3. \tag{3b}$$

Where θ_i is the phase of ith short. The reciprocity and the symmetry properties of the T-junction have been used in eq. (3). These are

$$S_{13}^2=S_{31}^2=S_{23}^2=S_{32}^2 \tag{4a}$$

$$S_{12}=S_{21} \tag{4b}$$

$$S_{11}=S_{22} \tag{4c}$$

and

$$S_{m11i}=S_{m22i} \tag{5a}$$

$$S_{m12i}=S_{m21i}. \tag{5b}$$

Solving (3a), S_{11}, S_{33} and S_{31}^2 can be obtained, and then substituting S_{33} and S_{31}^2 into (3b), S_{21} can be calculated.

B. T-Junction Scattering Parameter Modeling

Inspired by the three plane measurement method, three shorts (with different phases) are used to modify the T-junction configuration. Once the side-arm of the T-junction is shorted and regions 3 and 4 are combined to form region B in Fig. 1(b), this new region is considered a uniform waveguide of cross section $(a\times b_i)$, different from the cross section of regions A and C $(a\times b)$, and length d. The problem is therefore reduced to a waveguide discontinuity problem of three waveguides: two infinite waveguides A and C of cross section $a\times b$, separated by a length d of waveguide B of cross section $a\times b_i$. The same procedure as in the three plane measurement method is used to obtain the *S*-parameters of the T-junction, except that the *S*-parameters of the three two-port

networks are now computed by using mode-matching techniques instead of measurements by the network analyzer.

Consider a TE_{10} mode incident from $z < -d$ on the junction discontinuities at $z = -d$ and 0. Due to the presence of these discontinuities, reflected waves are generated in region A, transmitted and reflected waves in region B, and transmitted waves in region C. Because the discontinuities are in only the y-direction in the x-y plane, the fields in each region will have the same variation in the x-direction. In order to calculate the reflected and transmitted fields for each mode in each region, the total transverse fields in each region are expanded in terms of the appropriate waveguide modes in the region: For region A ($z \leqslant -d$),

$$\bar{E}_t = \hat{e}_{A1} e^{-\gamma_{A1}(z+d)} + \sum_i A_i \hat{e}_{Ai} e^{\gamma_{Ai}(z+d)} \tag{6a}$$

$$\bar{H}_t = \hat{h}_{A1} e^{-\gamma_{A1}(z+d)} - \sum_i A_i \hat{h}_{Ai} e^{\gamma_{Ai}(z+d)} \tag{6b}$$

For region B ($-d \leqslant z \leqslant 0$),

$$\bar{E}_t = \sum_j \hat{e}_{Bj}\left[B_j^+ e^{-\gamma_{Bj}z} + B_j^- e^{\gamma_{Bj}z}\right] \tag{7a}$$

$$\bar{H}_t = \sum_j \hat{h}_{Bj}\left[B_j^+ e^{-\gamma_{Bj}z} - B_j^- e^{\gamma_{Bj}z}\right] \tag{7b}$$

For region C ($z \geqslant 0$),

$$\bar{E}_t = \sum_k C_k \hat{e}_{ck} e^{-\gamma_{ck}z} \tag{8a}$$

$$\bar{H}_t = \sum_k C_k \hat{h}_{ck} e^{-\gamma_{ck}z} \tag{8b}$$

where $\hat{e}_{Ai}, \hat{h}_{Ai}, \gamma_{Ai}$; $\hat{e}_{Bj}, \hat{h}_{Bj}, \gamma_{Bj}$; and $\hat{e}_{Ck}, \hat{h}_{Ck}, \gamma_{Ck}$ are the transverse electric and magnetic eigen-fields and the propagation constants of the normal waveguide modes in the regions A, B, and C, respectively. By applying the boundary conditions that the tangential electric and magnetic fields be continuous at $z = -d$ and 0 and taking the inner products with orthogonality relations on the eigen-mode fields, the following infinite sets of linear equations in the unknown coefficients B_j^+ and B_j^- are obtained:

$$\sum_m \left[W_{lm} B_m^+ + X_{lm} B_m^-\right] = 2\langle \hat{e}_{A1}, \hat{h}_{Bl}^* \rangle \tag{9a}$$

$$\sum_m \left[Y_{lm} B_m^+ + Z_{lm} B_m^-\right] = 0 \tag{9b}$$

where

$$W_{lm} = e^{\gamma_{Bm}d} T_{lm} + e^{\gamma_{Bl}d} \langle \hat{e}_{Bl}, \hat{h}_{Bl}^* \rangle \delta_{lm} \tag{10a}$$

$$X_{lm} = -e^{-\gamma_{Bm}d} T_{lm} + e^{-\gamma_{Bl}d} \langle \hat{e}_{Bl}, \hat{h}_{Bl}^* \rangle \delta_{lm} \tag{10b}$$

$$Y_{lm} = T_{lm} - \langle \hat{e}_{Bl}, \hat{h}_{Bl}^* \rangle \delta_{lm} \tag{10c}$$

$$Z_{lm} = -T_{lm} - \langle \hat{e}_{Bl}, \hat{h}_{Bl}^* \rangle \delta_{lm} \tag{10d}$$

$$\langle \hat{e}, \hat{h}^* \rangle = \int_s (\hat{e} \times \hat{h}^*) . \hat{n} dS \tag{10e}$$

and

$$T_{lm} = \sum_i \left[\frac{\langle \hat{e}_{Ai}, \hat{h}_{Bm}^* \rangle}{\langle \hat{e}_{Ai}, \hat{h}_{Ai}^* \rangle}\right]^* \langle \hat{e}_{Ai}, \hat{h}_{Bl}^* \rangle. \tag{10f}$$

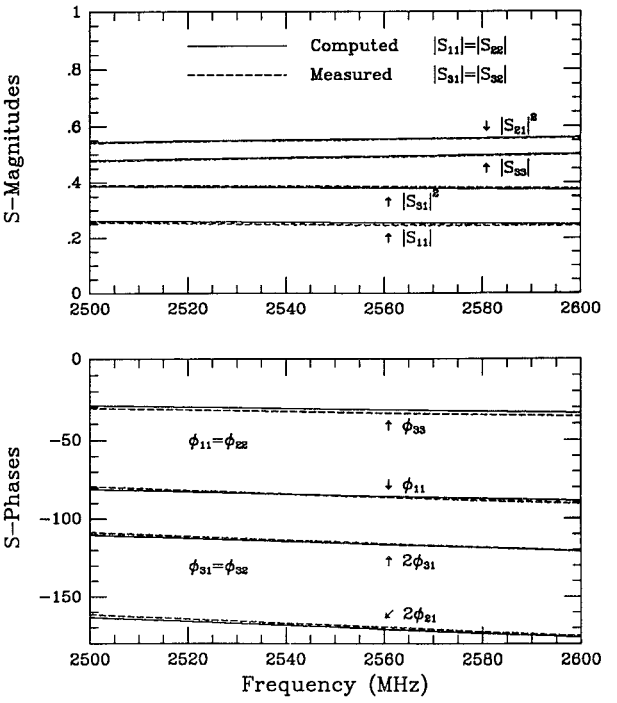

Fig. 3. Scattering parameters for an S-band E-plane T-junction with $a = 2b = 3.4$ inch, $d = b = 1.7$ inch.

The numerical solution of (9) for B_m^+ and B_m^- is achieved by truncating the infinite set to a finite number of equations. The A_i's and C_k's are given by

$$A_i = \delta_{i1} - \frac{\sum_j \left[B_j^+ e^{\gamma_{Bj}d} - B_j^- e^{-\gamma_{Bj}d}\right] \langle \hat{h}_{Bj}, \hat{e}_{Ai}^* \rangle}{\langle \hat{h}_{Ai}, \hat{e}_{Ai}^* \rangle} \tag{11a}$$

$$C_k = \frac{\sum_j \left[B_j^+ - B_j^-\right] \langle \hat{h}_{Bj}, \hat{e}_{Ck}^* \rangle}{\langle \hat{h}_{Ck}, \hat{e}_{Ck}^* \rangle}. \tag{11b}$$

Once the coefficients of the eigen-mode fields in each region are obtained, the incident and scattered waves on the equivalent multiport network (due to multi-modes) of the side-arm shorted T-junction are taken as proportional to the coefficients A_i and C_k, respectively. The proportionality constants are the normalization factors $\langle \hat{e}_{Ai}, \hat{h}_{Ai}^* \rangle$ or $\langle \hat{e}_{Ck}, \hat{h}_{Ck}^* \rangle$. Thus a two-port network shown in Fig. 2(b) can be used to characterize the discontinuity problem. Since regions A and C have the same cross sections the corresponding S-parameters are simply,

$$S_{11} = S_{22} = A_1 \tag{12a}$$

$$S_{21} = S_{12} = C_1. \tag{12b}$$

A computer program was developed to compute the S-parameters of both E-plane and H-plane rectangular waveguide T-junctions. Convergence of the solutions was checked by increasing the number of modes used in the

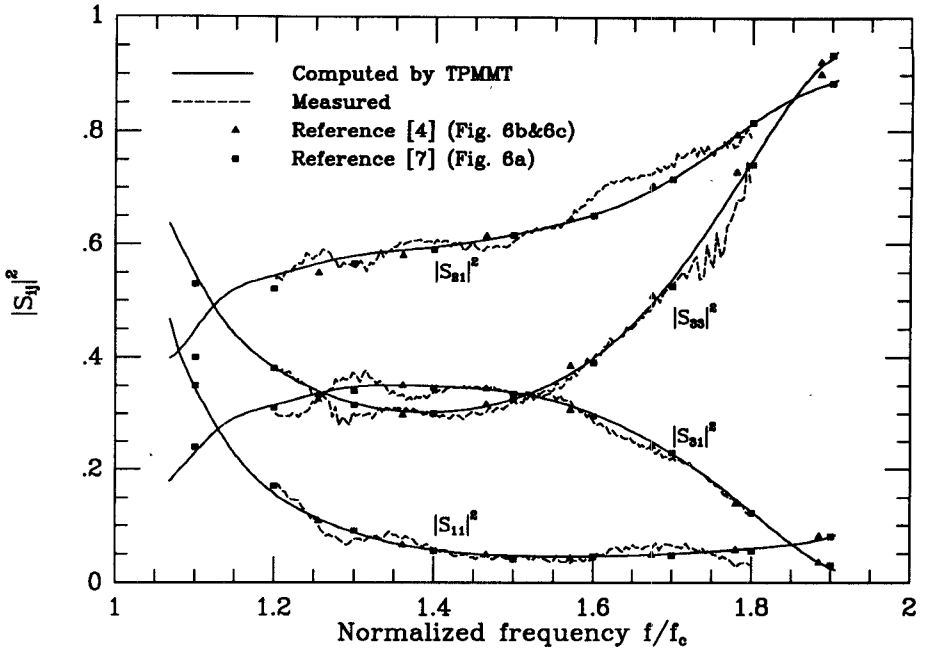

Fig. 4. Scattering parameters for an H-plane T-junction with $d = b = 2a = .9$ inch, $a = 45$ inch.

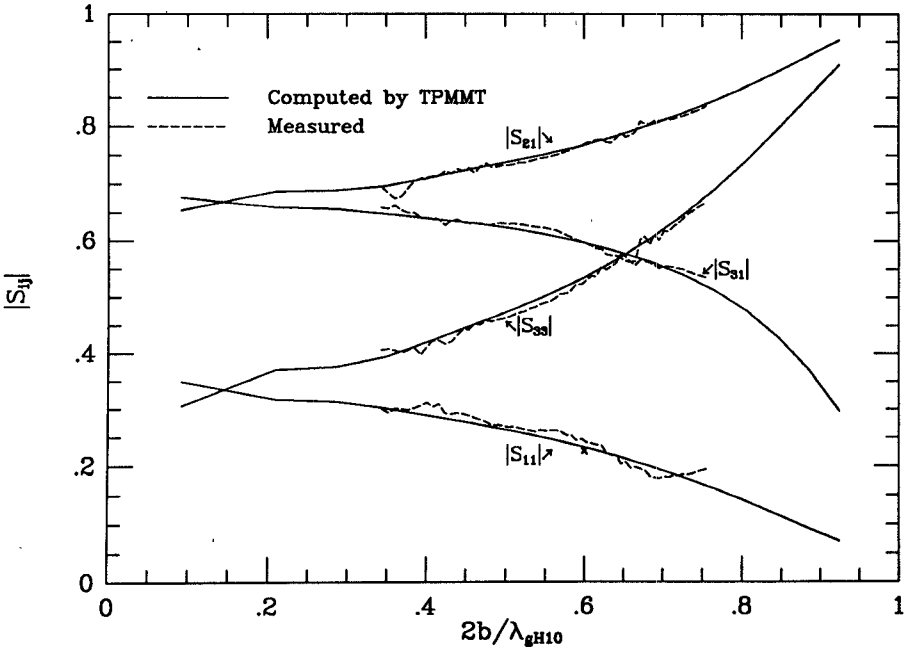

Fig. 5. Scattering parameters for an E-plane T-junction with $a = 2b = 3.4$ inch, $d = b = 1.7$ inch.

mode-matching techniques. Six modes in each region were found to be sufficient for convergence of the S-parameters to within 0.5%.

Using the three plane method, the best choice of lengths for the three shorts is to make the phase difference between each two of the three lengths $\pm 120°$. Considering the higher order modes excited by the T-junction, a certain minimum distance from the mouth of the T to the short is necessary to avoid higher order mode interaction between the short reference plane and the T-junction. On the other hand, the longer the minimum distance is, the more the number of modes in region B is needed. As a compromise, it is found that $(0.6-0.8)\lambda_g$ is the best choice for the minimum short circuit distance.

Fig. 3 shows the computed results by the TPMMT method, and the measured data from an HP8510B network analyzer, showing the magnitudes and the phases of an S-band E-plane T-junction over the frequency band from 2.5 to 2.6 GHz. Agreement between the computed and measured data is remarkable.

Fig. 4 compares the measured S-parameters of an H-plane T-junction with that computed by the TPMMT

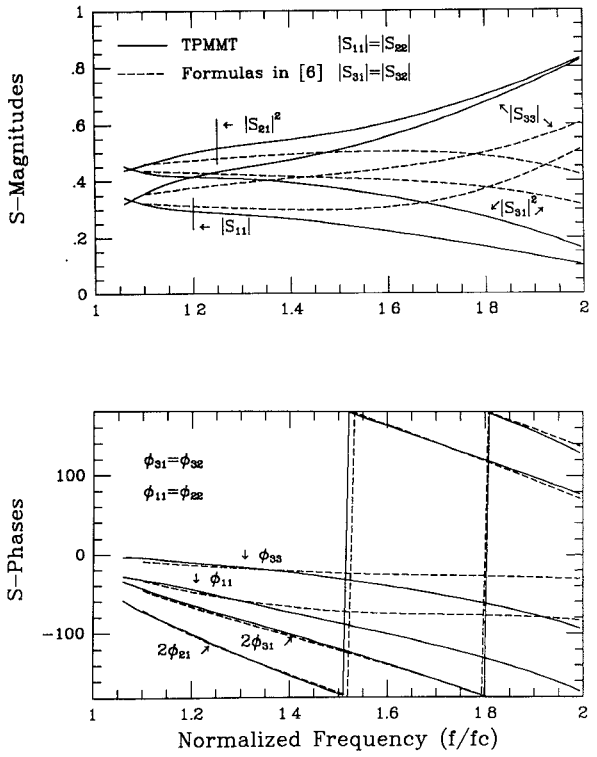

Fig. 6. Comparison between the results of TPMMT and equivalent circuit for E-plane T-junction with $a = 2b$, $d = b$.

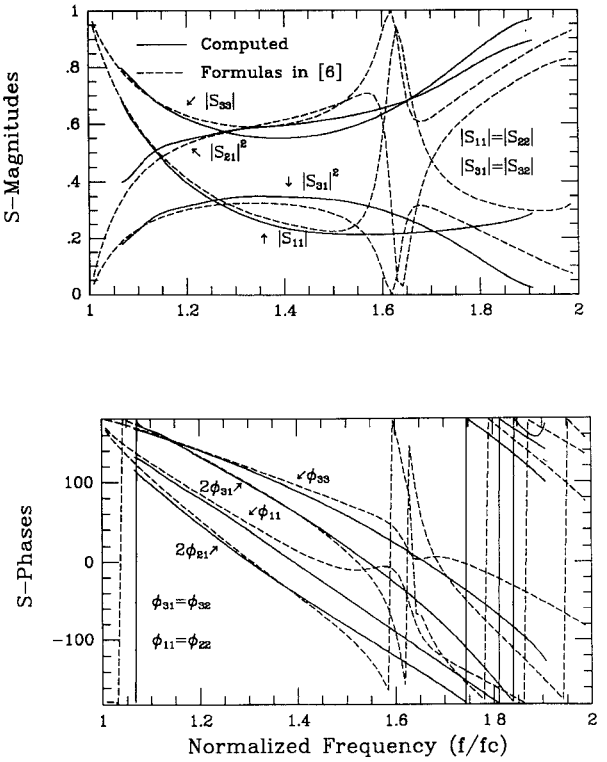

Fig. 7. Comparison between the results of TPMMT and equivalent circuit for H-plane T-junction with $b = 2a$, $d = b$.

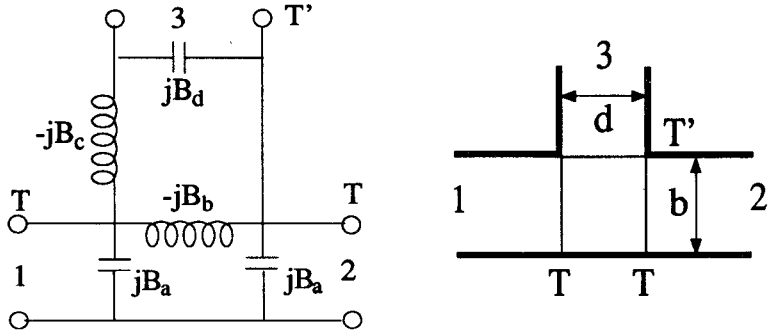

(a)

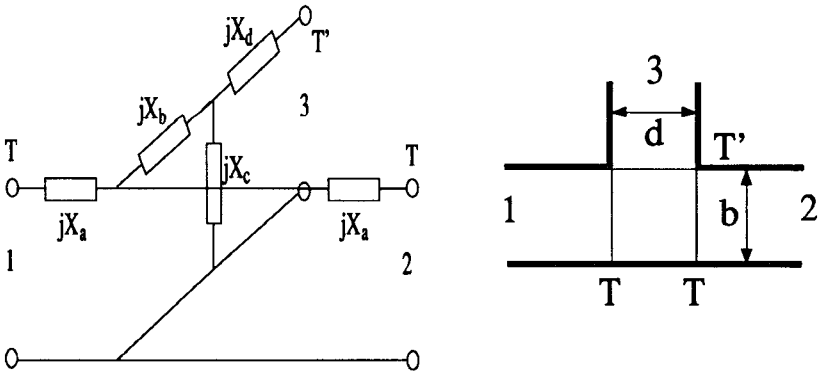

(b)

Fig. 8. T-junction equivalent circuits. (a) E-plane. (b) H-plane.

TABLE I
POLYNOMIAL COEFFICIENTS FOR E-PLANE T-JUNCTION WITH DIMENSIONAL PARAMETERS $a = 2b$, $d = b$

$k \backslash b's$	$b_0^{(k)}$	$b_1^{(k)}$	$b_2^{(k)}$	$b_3^{(k)}$	$b_4^{(k)}$	$b_5^{(k)}$	$b_6^{(k)}$
a	114.0511	−506.5494	920.1419	−878.7803	467.6217	−131.7710	15.4160
b	−13.1787	50.4164	−76.5400	57.7981	−21.6393	3.2407	—
c	560.9282	−2154.8618	3457.6345	−2957.0832	1419.8324	−362.6318	38.4726
d	−48.4935	216.9668	−398.1267	383.1617	−203.4954	56.5548	−6.4179

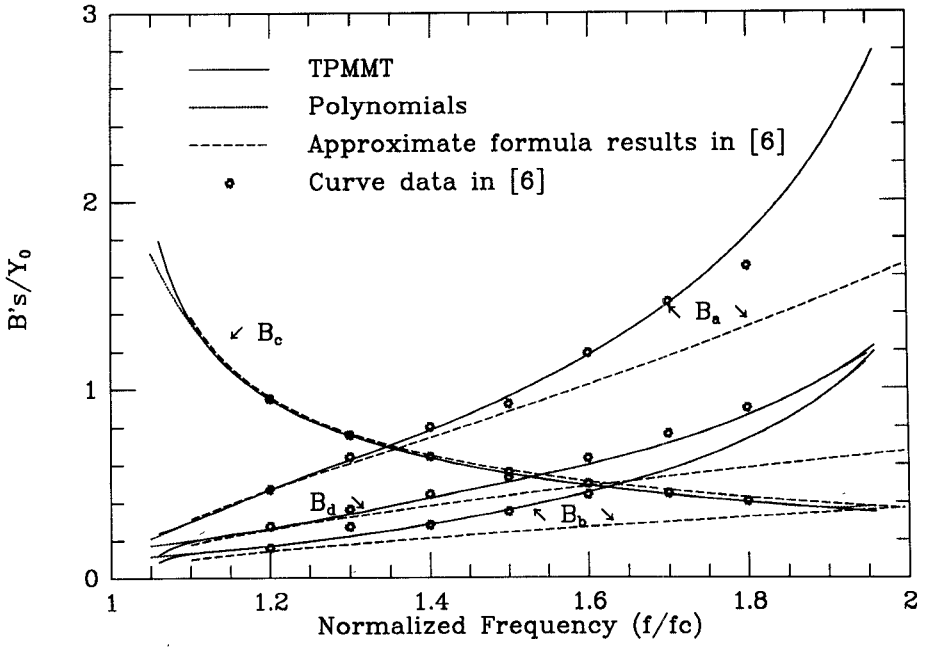

Fig. 9. Equivalent circuit parameters for E-plane T-junction with $a = 2b$, $d = b$.

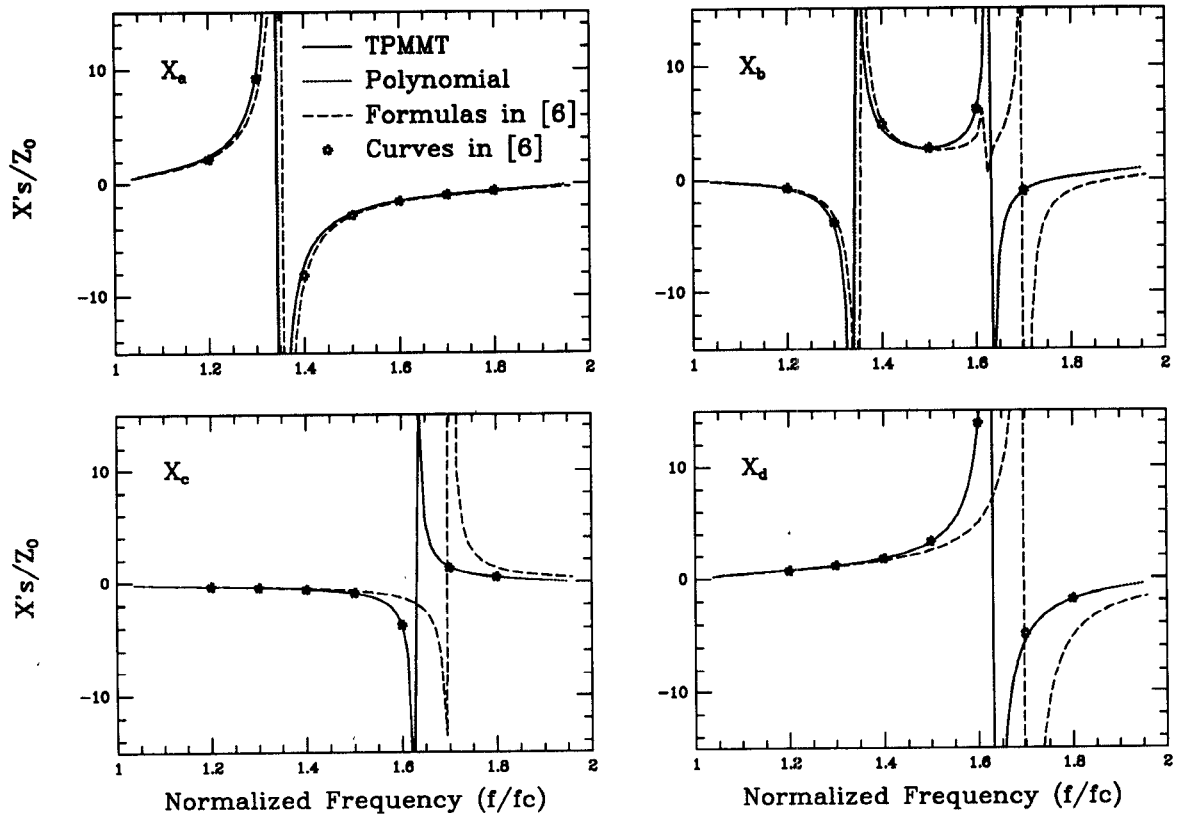

Fig. 10. Equivalent circuit parameters for H-plane T-junction with $b = 2a$, $d = b$.

TABLE II
POLYNOMIAL COEFFICIENTS AND POLES FOR H-PLANE T-JUNCTION WITH DIMENSIONAL PARAMETERS $b = 2a$, $d = b$

$k \backslash x's$	$x_0^{(k)}$	$x_1^{(k)}$	$x_2^{(k)}$	$x_3^{(k)}$	$x_4^{(k)}$	$x_5^{(k)}$	$x_6^{(k)}$	P_1	P_2
a	195.8846	−810.7328	1394.7536	−1276.3331	654.0399	−177.9816	20.0767	1.3417	—
b	−58.5277	249.8083	−442.8782	417.3045	−220.2853	61 7781	−7.1977	1.3417	1.6298
c	−104.2241	424.1251	−715.9226	642.8116	−323.8097	86.7534	−9.6568	1.6298	—
d	7.7803	−20.4710	21.0150	−11.0336	2.8589	−0.2650	—	1.6298	—

and other published methods [4], [7]. The results are in excellent agreement over the total waveguide frequency band.

Fig. 5 gives the performance of an E-plane T-junction over a total waveguide frequency band. The results computed by TPMMT and measurements are in agreement.

C. T-Junction Equivalent Circuit

The methods of waveguide T-junction characterization, including finite element, boundary element [7], Y-parameter [9] and the TPMMT methods solve the boundary value problems to obtain the scattering matrix of the three-port network. All these methods cannot be easily adopted and incorporated in microwave circuit CAD programs.

Although the present analysis is valid for any dimensional parameters, all the data and comparisons presented in this section are for $a = 2b$, $d = b$ for the E-plane and $b = 2a$, $d = b$ for the H-plane cases shown in Fig. 1(b).

Figs. 6 and 7 compare the S-parameters magnitudes and phases, obtained from the TPMMT and from the equivalent circuits [6] for E-plane and H-plane T-junctions, respectively. The curves for the equivalent circuit model were computed using approximate expressions given in [6] (i.e., (1) to (5) of Section 6.1 for the E-plane, and (1) to (4) of Section 6.5 for the H-plane. Note, however, that the parameter B in Section 6.5 has an error, it should be $B = (1/\pi)(1 + x^2)/(1 - x^2) + 0.3246)$.

Very accurate circuit model representations of E- and H-plane T-junctions may be derived by using topologies introduced by Marcuvitz [6], but the element values are derived from the TPMMT solutions. The element values are given in terms of simple polynomials or rational functions of the normalized frequency variable $\Omega = (f/f_c)$ where f is the frequency and f_c is the cut-off frequency of the TE_{10} fundamental mode in the waveguide. The circuit models of the E- and H-plane T-junctions introduced by Marcuvitz [6] are shown in Fig. 8(a) and (b), respectively. The scattering matrix elements of each of the T-junctions are computed by TPMMT as a function of the normalized frequency Ω. At each Ω, the element values of the circuit of Fig. 8(a) and (b) are derived from the scattering matrix.

For the E-plane T-junction, the three-port Y-parameters are computed from the scattering matrix $[S]$ using the relation $[Y] = ([I] - [S])([I] + [S])^{-1}$, where $[I]$ is the unit matrix. The element values of the equivalent circuit in Fig. 8(a) are then easily shown to be given by

$$jB_c = y_{31} \tag{13a}$$

$$jB_b = y_{21} - jB_c \tag{13b}$$

$$jB_a = y_{11} + jB_b + jB_c \tag{13c}$$

$$jB_d = y_{33} + jB_c. \tag{13d}$$

Each of the element values B_a, B_b, B_c and B_d of Fig. 8(a) are expressed as a sixth order polynomial in Ω:

$$B_k(\Omega) = \sum_{i=0}^{6} b_i^{(k)} \Omega^i \tag{14}$$

where $k = a, b, c, d$. The coefficient $b_i^{(k)}$ are obtained by fitting the element values obtained from the scattering matrix to expressions (14) with the mean square regression method. Table I gives the polynomial coefficients $b_i^{(k)}$. Fig. 9 compares the circuit element values obtained from the TPMMT, the polynomial approximations (14), the approximate expressions and the curves of reference [6] (Figures 6.1–4 to 6.1–7 in [6]).[1] The data from the curves in [6] are very accurate, it is not clear, however, how the curves were generated.

For the H-plane T-junction a similar procedure is used. The three-port Z-parameters are computed from the scattering matrix using the relation $[Z] = ([I] + [S])([I] - [S])^{-1}$. The element values of the equivalent circuit in Fig. 8(b) are given by

$$jX_c = z_{31}. \tag{15a}$$

$$jX_b = z_{21} - jX_c \tag{15b}$$

$$jX_a = z_{11} - jX_b - jX_c \tag{15c}$$

$$jX_d = z_{33} - jX_c. \tag{15d}$$

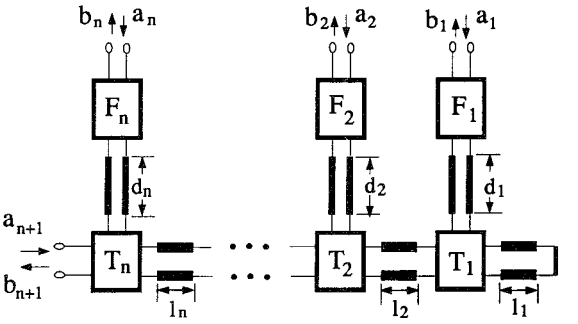

Fig. 11. n-channel multiplexer network.

[1] Note that there is an error in labeling the parameters of these curves in [6]. The parameter b/λ_g shown in the curves should read $2b/\lambda_g$.

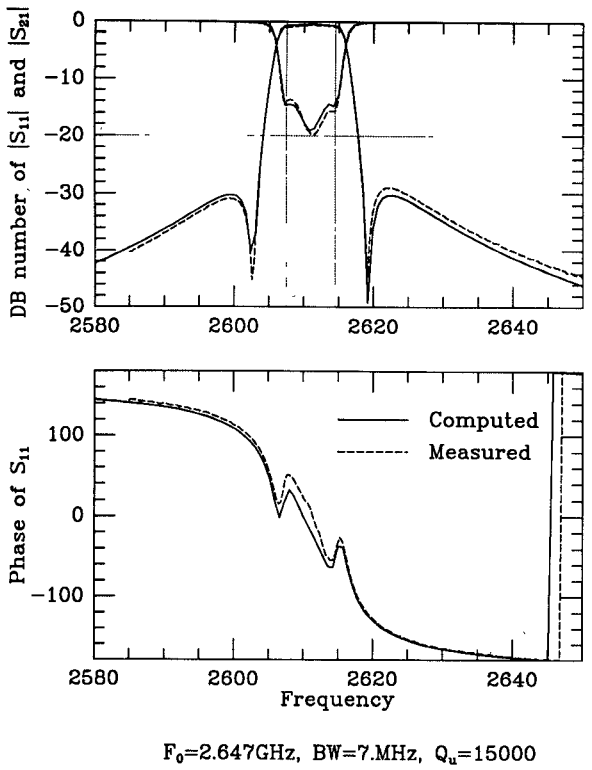

Fig. 12. Individual filter response for a typical channel.

The reactance element values X_a, X_b, X_c and X_d of Fig. 8(b) are expressed as rational functions of the normalized frequency Ω:

$$X_k(\Omega) = \sum_{i=0}^{6} x_i^{(k)} \Omega^i / (\Omega - P_1) \qquad (16)$$

where $k = a, c, d$; and

$$X_b(\Omega) = \sum_{i=0}^{6} x_i^{(b)} \Omega^i / [(\Omega - P_1)(P_2 - \Omega)]. \qquad (17)$$

Fig. 10 compares the variation of the circuit element values for the H-plane T-junction. Table II gives the polynomial coefficients $x_i^{(k)}$ and the poles P_1 and P_2.

III. Multiplexer Model and Optimization

The n-channel multiplexer shown in Fig. 11 consists of a waveguide manifold and n band-pass filters connected to it through n waveguide T-junctions. Methods for the analysis, optimization and design of such multiplexer are described in [1]–[3]. The practical success of the multiplexer designs are critically dependent on the accuracy of the models used to compute the frequency dependence of the filter and T-junction scattering parameters. Typically measured S-parameters of the T-junctions are used, together with a circuit model of the filters to model the multiplexer response. Computer optimization routines are then employed to find optimum values of the manifold spacings l_k and d_k (shown in Fig. 11), as well as the filter parameters. When a satisfactory computer optimized solution is achieved, it usually takes several experimental steps to practically obtain the same result. We used the T-junction model developed in the previous section, together with a modified circuit model of the filters described in [1] to design a four channel S-band multiplexer. After the computer optimization had been performed, the four filters were designed, built, tuned, and tested individually. The waveguide manifold was also built with the optimized dimensions. The four channel multiplexer was then assembled and tested *without any further tuning*. The result was extremely close to the computer design.

Fig. 12 shows typical computed results superimposed on the measured individual filter characteristics (both magnitude and phase of the reflection coefficient are shown). The filters used initially, before optimization, are doubly terminated four-pole elliptic function filters with .05 dB pass band ripple and 30 dB minimum out of band rejection. Fig. 13 shows the computed optimized multiplexer response, while Fig. 14 shows the measured multiplexer response.

IV. Conclusion

A rigorous method is presented to model rectangular waveguide T-junctions. The method is a combination of mode-matching and a three plane measurement method. The computed and measured results of magnitude and phase of the scattering matrix elements are in excellent agreement for both E-plane and H-plane T-junctions. The equivalent circuit models for both E-plane and H-plane T-junctions are used with their parameters derived from the electromagnetic model. These parameters are represented by polynomials and they provide very good accuracy (less than 1% magnitude error and less than 2° of phase error of the scattering parameters).

The optimization procedure of the multiplexer network model gives very good design of the manifold and the filters of the multiplexer. An experimental multiplexer built in accordance with the optimized design shows remarkable agreement with the theoretical results, without any additional tuning.

The TPMMT may also be used to solve other problems which have field deficiencies in some regions, such as right angle bends in waveguides, T-junction series, etc.

Acknowledgment

The authors wish to acknowledge the extremely thorough, helpful and constructive comments by the reviewers, who suggested numerous improvements. The authors are grateful to Prof. A. Oliner for many valuable suggestions and discussions.

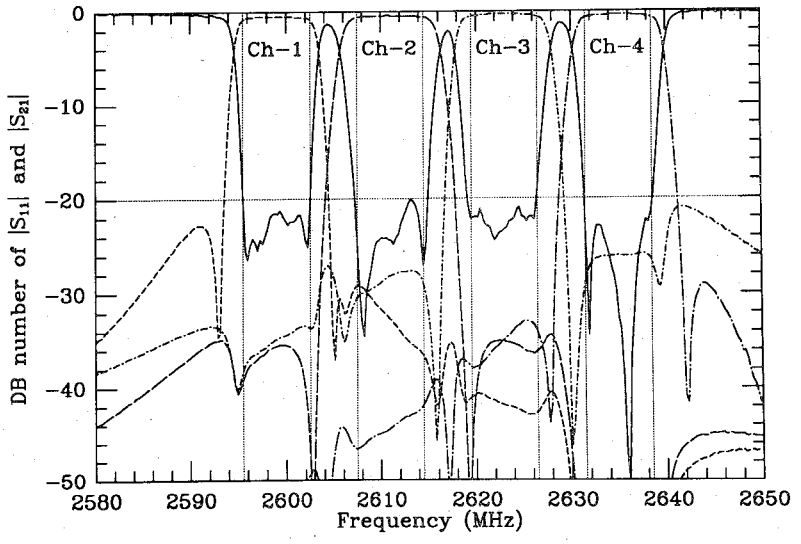

Fig. 13. Computed 4-channel multiplexer response.

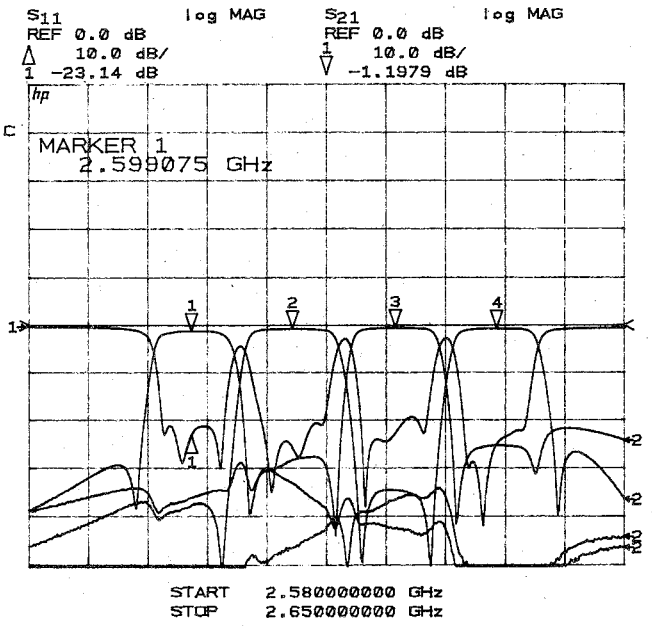

Fig. 14. Measured 4-channel multiplexer response.

References

[1] A. E. Atia, "Computer-aided design of waveguide multiplexers," *IEEE Trans. Microwave Theory Tech.*, vol. MTT-22, pp. 332–336, Mar. 1974.

[2] J. D. Rhodes and R. Levy, "Design of general manifold multiplexers," *IEEE Trans. Microwave Theory and Tech.*, vol. MTT-27, pp. 111–123, Feb. 1979.

[3] R. G. Egri, A. E. Williams, and A. E. Atia, "A contiguous-band multiplexer design," in *IEEE MTT-S Int. Microwave Symp. Dig.*, 1983, pp. 86–88.

[4] J. Dittloff and F. Arndt, "Rigorous field theory design of millimeter-wave *E*-plane integrated circuit multiplexers," *IEEE Trans. Microwave Theory Tech.*, vol. MTT-37, pp. 340–350, Feb. 1989.

[5] F. Arndt *et al.*, "Optimized *E*-plane T-junction series power dividers," *IEEE Trans. Microwave Theory Tech.*, vol. MTT-35, pp. 1052–1059, Nov. 1987.

[6] N. Marcuvitz, *Waveguide Handbook*, Radiation Laboratory Series, vol. 10, New York: McGraw-Hill, 1951.

[7] M. Koshiba and M. Suzuki, "Application of the boundary-element method to waveguide discontinuities," *IEEE Trans. Microwave Theory Tech.*, vol. MTT-34, pp. 301–307, Feb. 1986.

[8] L. Lewin, "On the inadequacy of discrete mode-matching techniques in some waveguide discontinuity problems," *IEEE Trans. Microwave Theory Tech.*, vol. MTT-18, pp. 364–372, July 1970.

[9] E. D. Sharp, "An exact calculation for a T-junction of rectangular waveguides having arbitrary cross sections," *IEEE Trans. Microwave Theory Tech.*, vol. MTT-15, pp. 109–116, Feb. 1967.

Xiao-Peng Liang (S'90) was born in Shanxi, China, in 1960. He received the B.S. and M.S. degrees in Beijing Institute of Technology, Beijing, China, in 1982 and 1984, respectively, both in electrical engineering.

From 1984 to 1987, he worked in Electrical Engineering Department, Beijing Institute of Technology, as a faculty member, where his research dealt mainly with the six-port measurement technique. He is presently a graduate student in the Electrical Engineering Department, University of Maryland at College Park, working towards the Ph.D. degree. His research interests are in the area of modeling microwave and millimeter-wave waveguides, devices and circuits.

Kawthar A. Zaki (SM'85–F'91), for photograph and biography see this issue page 2076.

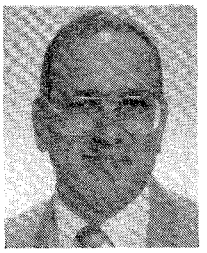

Ali E. Atia (S'67–M'69–SM'78–F'87) received the B.S. degree from Ain Shams University, Cairo, Egypt, in 1962, and the M.S. and Ph.D. degrees from the University of California, Berkeley, in 1966 and 1969, respectively, all in electrical engineering.

Prior to joining COMSAT in 1969, he held various research and teaching positions at both these universities. As a Senior Scientist in the Microwave Laboratory at COMSAT Laboratories, he has made original contributions to satel-

lite transponder and antenna technologies, most notably the development of the dual-mode microwave filters technology. He has also made significant contributions to several satellite programs, including INTELSAT IV-A, V, V-A, VI, ARABSAT, and AUSSAT. He was responsible for the design, implementation, qualification, and testing of major subsystems in COMSAT's NASA ATS-F propagation experiment and the COMSTAR Ka-band beacon experiment. As Senior Director in COMSAT Systems Division he was responsible for communications systems design, integration, implementation, and testing under contracts with various government and commercial customers. Presently he is Vice President and Chief Engineer for COMSAT Systems Division, Clarksburg, MD.

Dr. Atia is an Associate Fellow of the AIAA and a Member of Sigma Xi.